AD-A083 758 MISSOURI UNIV-ROLLA DEPT OF PHYSICS F/G 20/12
OPTICAL STUDIES OF THE INTERFACE STATES AT GAAS-METAL SCHOTTKY --ETC(U)
1980 R J BELL, R W ALEXANDER, G P ALLDREDGE AFOSR-76-2938

UNCLASSIFIED AFOSR-TR-80-0160 NL

1 OF 1
AD
A083758

END
DATE
FILMED
6-80
DTIC

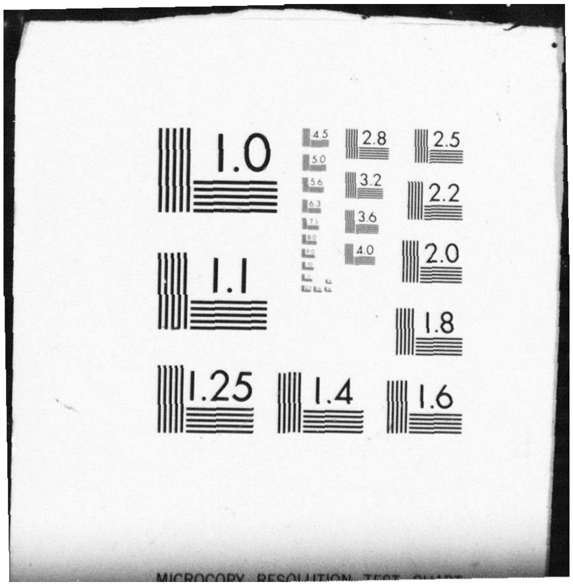

MICROCOPY RESOLUTION TEST CHART

(2) LEVEL II

See 1473

FINAL REPORT
AFOSR 76-2938

Optical Studies of the Interface States at GaAs-Metal Schottky Barrier Junctions

Robert J. Bell, Ralph W. Alexander, Jr., and Gerald P. Alldredge

Department of Physics
University of Missouri-Rolla
Rolla, Missouri 65401

DISCLAIMER NOTICE

Contents

I. Introduction

The goal of the proposal research was to study surface states at GaAs-metal Schottky barrier junctions and the effect of oxygen exposure on the surface states. It was proposed to use optical absorption measurements, photoelectric measurements, capacitance-voltage and conductance-voltage measurements with the goal of correlating the optical and electrical results.

For the most part, these goals have been reached. The optical measurements were unsuccessful in detecting the surface states, while the electrical measurements have provided interesting results. GaAs single crystals were cleaved in ultra high vacuum ($\sim 10^{-9}$ Torr) and either immediately metallized or first exposed to oxygen and then metallized. For aluminum metallization, for example, considerable differences were found between junctions formed with and without oxygen exposure. Oxygen caused a considerable increase in the surface state density and these additional surface states showed considerable frequency dispersion. Fortunately, from the device point of view, a large fraction of these oxygen-induced surface states are slow, so that high speed performance will not be completely degraded.

II. Optical Measurements

An attempt was made to observe the optical absorption due to the oxygen-induced surface states using a multiple internal reflection technique. This had been done successfully for Si and Ge.[1,2,3] Samples metallized with Al with and without oxygen exposure were compared, but no differences could be detected.

Photoelectric response measurements were also made on these samples, both internal (illuminated from the GaAs side) and external (illuminated from the Al side). The Fowler theory predicts that the photo current per absorbed photon, R, should be[4]

$$R \sim (h\nu - h\nu_o)^2 \qquad (1)$$

where $h\nu_0$ is the band gap energy. Any structure below $h\nu_0$ may be due to surface states. This has been seen in Si-metal junctions[5]. A plot of $R^{1/2}$ versus $h\nu$ can be used to obtain the barrier height:[4]

$V_B = .80 \pm .05$ ev for Al-GaAs

$V_B = .89 \pm .05$ ev for Ag-GaAs

Figure 1 shows $\sqrt{R}$ plotted versus $h\nu$ for Al-GaAs and Ag-GaAs diodes. However, no structure below the band gap indicative of surface states was seen in the samples studied. The reason for this is not known, as the electrical measurements suggest a sufficient density of surface states to be seen photoelectrically if the absorption cross section is similar to those observed for Si.

An interesting feature was noticed while making the optical measurements. The transparency of the samples varied widely from supplier to supplier and even within samples from the same supplier. Samples obtained from Monsanto were opaque in the 1-2 μm region, most samples from Morgan Semiconductor were also highly absorbing, while most samples from Laser Diode were transparent. The reason for the great differences in the infrared transparency has not been explored. However all our measurements were made on transparent samples, the majority from Laser Diode Loboratories. It would be interesting to see if device yield or characteristics correlates with the infrared transparency.

III. Electrical Measurements

Diodes were prepared on freshly cleaved (110) surfaces, with and without oxygen exposure, before vapor deposition of either gold or aluminum. Before the samples were mounted in the UHV chamber for cleaving, ohmic contacts were made by diffusing tin contacts in an H_2 and HCl atmosphere at a temperature of 300C for 1 minute. To obtain samples with minimal oxygen exposure, single crystals were cleaved in a metal vapor stream at a pressure of about 10^{-9}

Torr. Oxidized samples were obtained by cleaving in UHV and then exposing the sample to oxygen or air at one atmosphere for one hour. This should give an equilibrium oxide layer typical of device manufacturing conditions.[6] Only cleaves yielding large smooth areas were used.

The forward current density is related to the applied voltage by[4]

$$J \sim \exp\left(\frac{qV}{nkT}\right) \tag{2}$$

where n is the ideality parameter

$$n \equiv \frac{q}{kT} \frac{\partial V}{\partial (\ln J)} \tag{3}$$

The parameter n is sensitive to surface treatment and disorder.[7] For our samples without oxygen exposure n was typically about 1.1, while samples exposed to oxygen had larger values of n, about 1.5. Figures 2(a) and 2(b) show the I-V characteristics for an Al-GaAs diode which had been exposed to O_2 after cleaving and before metallization. The dashed line in Fig. 2b gives $n \simeq 1.5$. Amith and Mark[7] have studied GaAs metal diodes to look for effects of oxygen and surface disorder. However, they did not start with a clean, cleaved surface. Instead, they ion sputtered and then annealed. The clean, ordered (as determined by LEED) surface gave values of n greater than three, while dirty, disordered or oxidized surfaces gave $n \sim 1.35 - 1.5$. A comparison of these results with ours suggests that their method of preparing a clean surface gives a surface quite different in some way from that obtained by an UHV cleave. Quite likely, the stoichciometry of their surface differs from the ideal despite good LEED patterns.

An estimate of the barrier heights V_B can also be obtained from the I-V curve. Good agreement was found with the values obtained from the photo response for our diodes.

The capacitance and conductance was measured as a function of applied bias and frequency between 5kHz and 20kHz using a Boonton 1615A bridge and a lock-in amplifier as a detector. Some measurements were made at higher frequencies, but errors in the bridge reduced the accuracy of these.

In the reverse bias region, the slope of $(\frac{1}{c})^2$ vs. V is related to the bulk impurity concentration by[4]

$$N_D = \frac{2}{qE_sA^2} \frac{dv}{d(1/c^2)} \tag{4}$$

where E_s is the dielectric constant of GaAs, q is the electron charge and A the area of the diode.

To analyze the capacitance-voltage data, two models were used: one for the clean, UHV cleaved surfaces and one for the oxidized surfaces. For the clean surface, the equivalent circuit shown in Fig. 3a was used.[8] The observed absence of frequency dispersion in the conductance was taken as evidence of the validity of this model for clean surfaces. Deneuville[8] used this model to extract the density of surface states from C-V measurements on Si diodes.

For the oxidized samples, the equivalent circuit shown in Fig. 3c was used. Kar and Dahlke[9] used this model to analyze the surface states for Si diodes. It shows large frequency dispersion of the measured admittance caused by carrier recombination in interface states.

Figure 4 shows the conductance versus bias voltage for Al-GaAs diodes with oxygen exposure before deposition of the Al electrode for several frequencies. Considerable frequency dispersion for the oxidized surface is seen, while essentially no frequency dispersion of the conductance was seen for diodes without oxygen exposure.

Several steps are involved in analyzing the measured capacitance data. The bridge gives the series capacitance, C_s and series conductance as shown in Fig. 5 (a). Following Kar and Dahlke[9], this is changed to the equivalent circuit shown in Fig. 5(b), where

$$C' = \frac{C_s}{1+D^2}\ , \ G' = C'\omega D \tag{5}$$

To account for the resistance in the substrate, this is modeled by the circuit shown in Fig. 5(c) with

$$C_m{}'(\omega) = \frac{C'}{(1-RG')^2 + \omega^2 R^2 C'^2} \tag{6}$$

and

$$G_m{}'(\omega) = \frac{G' - R(G'^2 + C'^2\omega^2}{(1-RG')^2 + \omega^2 R^2 C'^2} \tag{7}$$

where R is the series resistance of the substrate. R can be found as the inverse of the saturation value of G' in the forward bias region. One now pictures the diode current as coming from two contributions, one from tunneling through the oxide layer (largely frequency independent) and one from recombination at the interface. This is shown in the equivalent circuit of Fig 5(d). G_T is the frequency independent tunneling contribution to the conductance and

$$\begin{aligned} G_{a,c}(\omega) &= G_m{}'(\omega) - G_T \\ &\simeq G_m{}'(\omega) - G_{dc} \text{ if } G_{dc} << \frac{1}{R} \end{aligned} \tag{8}$$

G_{dc} can be obtained by graphically differentiating the static I-V curve. The next step is to break the capacitance into a contribution due to the oxide barrier C_{ox} in parallel with a capacitance, C_p, (ω) representing the surface state capacitance and the space charge capacitance. The resulting equivalent circuit is shown in Fig. 5(e) and[10]

$$C_p(w) = \frac{C_{ox}(G_{ac}{}^2 + \omega^2 C_m{}^{12})[\omega^2 C_m{}^1(C_{ox} - C_m\ ) - G_{ac}{}^2]}{\omega^2 C_{ox}{}^2 G_{ac}{}^2 + [\omega^2 C_m{}'(C_{ox} - C_m{}') - G_{ac}{}^2]^2} \tag{9}$$

$$G_p(w) = \frac{\omega^2 C_{ox}{}^2 G_{ac}(G_{ac}{}^2 + \omega^2 C_m{}'}{\omega^2 C_{ox}{}^2 G_{ac}{}^2 + [\omega^2 C_m{}'(C_{ox} - C_m{}') - G_{ac}{}^2]^2} \tag{10}$$

C_{ox} is equal to the saturation capacitance, C_s, in Fig. 5a in the strong accumulation region. Our final step is to put the space charge capacitance in parallel with surface state capacitance C_s as shown in Fig. 3c. The space charge capacitance is[4]

$$C_{sc} = A\sqrt{\frac{q\varepsilon_s N_D}{2(V_D - V)}} \tag{11}$$

where A = the diode area
q = the electron charge
ε_s = the dielectric constant of GaAs
N_D = the doping concentration
V_D = the conduction band bending
V = the bias voltage

At low frequencies, that is those frequencies for which the surface states relax rapidly compared to the frequency, Fig. 5(e) becomes Fig. 6(b). The capacitance due to the surface states, C_s, can be found from

$$C_s = C_p(\omega_{eq}) - C_{sc} \tag{12}$$

and the density of surface states from

$$N_{ss} = \frac{C_s}{qA} \tag{13}$$

Figure 7 shows the three terms in eq. (12), namely $C_p(\omega_{eq})$, C_{sc} and C_s, for an oxygen exposed Al-GaAs diode. The density of surface states derived from these curves is shown in Fig. 8. It can be seen that there is a peak in the density of surface states at about 0.28 ev above the Fermi level.

The density of free carriers in the bulk derived from the $1/c^2$ vs. V curve [eq. (4)] was 2.3×10^{16} cm^{-3} in reasonable agreement with a Hall measurement of N_D supplied by the manufacturer.

Figure 9 shows the forward biased I-V curve for Al-GaAs metallized immediately after an UHV cleave. The ideality factor n is found to be 1.1, as compared to $n \sim 1.5$ for a diode formed with O_2 exposure before metallization. Figure 10 shows the C-V curves for the clean Al-GaAs diode. Note that the peak in C' is at about 0.2 ev above the Fermi level and considerable reduced in size from the oxygen-exposed diode. Also, the frequency dispersion is much less for the clean sample than for the oxygen-exposed sample (Fig. 7). Clearly, the presence of O_2 has created more surface states, and these surface states have relatively long relaxation times.

Figures 11 and 12 show I-V and C-V curves for Ag-GaAs diodes with oxygen exposure before metallization. The peak in the density of surface states is now at about .3 ev above the Fermi level, and again the surface density is considerably reduced compared to the Al-GaAs dioxide with O_2 exposure.

For Au-GaAs diodes with oxygen exposure, the peak in the density of states shifts further above the Fermi level to about 0.45 ev. The I-V curve for one of these diodes is shown in Figure 13.

Measurements are currently being analyzed for the Au-GaAs diodes without oxygen exposure.

IV. Quantum-Mechanical Calculations Relating to the Metallization of the Surfaces of GaAs, Particularly the Pt/GaAs Interface

A. Introduction

The work of this part was the responsibility of one of the principal investiators, G. P. Alldredge, with the assistance of C. A. Ward.

The primary aim of this subtask was the investigation of the electronic structure of the GaAs surface in interaction with metallizing atoms and the exploration of the resultant atomic geometries. The results of such studies are expected to give information on formation of intermetallic compounds, on diffusion barriers, and on other details of atomic geometry in junction regions of GaAs devices. Such results yield insights that are useful in attacking such practical problems as the stability of Schottky barriers in devices operating at high power levels for extended times. Additionally, the electronic structure itself, evaluated at minima of the calculated potential surfaces, is of importance in interpreting experimental electron spectroscopies being applied in other laboratories to study GaAs interface problems.

A second aim developed during the course of the grant period when attention became focussed on certain intermetallic crystal compounds which were identified in experimental studies of metal/GaAs interfaces. This aim was to investigate the bulk electronic band-structure of some of those compounds whose band-structure was not well known. $PtAs_2$, in the pyrite structure, is an example of such crystal compounds of interest. To support these primary aims, two important secondary aims were identified very early in the grant period. One was the task of providing the necessary software for large-scale computation of the kind needed for the primary aims. The second was the testing on simplified programs of new computational techniques needed, some of which provided in results that are interesting in their own right.

The following subsection summarizes the work accomplished toward meeting these aims. It will be seen that work remains to be done to meet the primary aims. Considerably greater success was attained in meeting the secondary aims.

B. Work Carried Out and In Progress

1. LCMTO thin-film study of electronic structure of Pt on GaAs (110). Alldredge, in collaboration with L. Kleinman[11], was the first worker to calculate the electronic structure of a bare metallic surface using a psendopotential method with realistic boundary conditions, and (with the further collaboration of E. Caruthers) this method was used to investigate several problems.[12,13] However, it was felt that a method better adapted to a treatment of d-states than a psendopotential should be used to treat the Pt/GaAs(110) system. Accordingly, a collaboration with R. V. Kasowski (DuPont Research Laboratory) was initiated, utilizing the technique of linear combination of muffin-tin orbitals (LCMTO), especially as applied to thin films[14].

This collaboration consisted both of exploratory calculations carried out at DuPont and of a conversion of Kasowski's initial LCMTO codes from their original Univac 1100 and DEC PDP-10 forms to an IBM S/370 form to run at the University of Missouri. The conversion project was a massive one. The original LCMTO code was a suite of about a dozen programs, comprising some 20,000 lines of Fortran.

Preliminary results were obtained for a GaAs (110) film with Pt atoms placed in a bonding position with respect to the surface As atoms. When only 5d orbitals are allowed as basis functions for the Pt valence electrons, the results for energy levels looked encouraging, although obviously not complete since it is well known that the Pt crystal has about one s valence electron per atom. When 6s orbitals were included in the basis for Pt, difficulties arose with so-called "over-completeness" (i.e., near linear dependence) of the MTO basis set.

At this point, we had to re-evaluate the prospects for this method. The problem with linear dependence of the basis set including 6s orbitals for Pt could be solved satisfactorily and rather straightforwardly. A tougher problem was presented by the large computer time requirements. Because of this requirement of still further development of the LCMTO suite, it was decided to temporarily abandon this approach for the purpose of the present grant, and to look to cluster methods for an alternate approach. In addition, it was clear that much more careful attention would have to be given to means of accelerating the rate of convergence to self-consistency over the usual methods used in bulk electronic band-structure. This concern led us to use a semiempirical quantum-chemical method, the modified intermediate neglect of diatomic overlap method (MINDO/3), as a model for experimenting with improvements in scf convergence: These experiments have met with some success, and the results will be detailed in subsection 4 below.

2. Cluster simulation of interface systems. When it became clear that the LCMTO code for thin films still required extensive development work for the reasons discussed in the preceding subsection, we decided to implement two complementary methods for simulating interface systems by moderately large clusters of substrate units with overlayer atoms in contact with them. The two methods chosen were the multiple-scattering $X\alpha$ self-consistent (MS-$X\alpha$-SCF) method[15] and the linear-combination-of-atomic-orbitals $X\alpha$ self-consistent (LCAO-$X\alpha$-SCF) method.[16] While we began with the MS-$X\alpha$-SCF, we believe it is necessary to work with both techniques more or less in parallel. At their present state of development neither is a complete method (even within the $X\alpha$ form of the local density functional approximation), and the strong points of each tend to compensate for the weak points of the other. For example the muffin-tin approximation which makes the MS-$X\alpha$ method so fast introduces some uncertainty in the physical applicability of its results, especially with respect to determination of the variation of total

energy with geometry.[17] Allowing overlap of the muffin-tins permits a significant reduction in the uncertainty, but at the expense of a certain degree of empiricism in determining the degree of overlap.[18] On the other hand, the LCAO-Xα method avoids the muffin-tin procedure and its associated uncertainties, and it does provide solutions which (for given values of α) are variational in character and gives total energies without the trouble of additional parameters of the character of the muffin-tin radii. But to be competitive in speed, the LCAO-Xα method requires choices of basis functions (the AOs and fitting functions for the charge ane exchange-energy densities) which try to strike a delicate balance between a limited number of functions in a basis set and as much variational flexibility as feasible. Thus, an investigation of a physical problem which makes use of both methods in parallel whould be on much firmer ground than either separately.

To use the MS-Xα-SCF method, we have implemented and tested two independently-coded sets of programs: (1) the University of Florida suite MUSCATEL,[19a] and (2) the very recently released University of Manitoba program MSXALF.[19b] Troubling discrepancies in results on a benchmark system obtained from a program similar to MUSCATEL[20] and from MSXALF appear to be partially explained in terms of inadequate approximations for overlap integrals in the earlier program.[21] Work is now underway toward calculating electronic structure of GaAs clusters, with current attention focussing on two problems: (1) investigating the effects of terminating that part of the cluster which would be connected to the rest of the solid if we were able to truly treat a semi-infinite substrate; and (2) investigating the sensitivity of geometrical dependence of the total energy on the various choices of muffin-tin radii and their degrees of overlap. Some of this work is being continued at UM-Columbia beyond the termination of this grant.

The major part of an LCAO-Xα-SCF program suite is now in hand, and we are now working toward the complete implementation and testing of this technique.

3. Electronic structure of $PtAs_2$. The LCMTO work of 1.) and the cluster calculations of 2.) above do not take into account relativistic effects. Even more strongly than spin-orbit effects which will cause splitting of many degeneracies, the relativistic Darwin and mass-velocity effects in compounds containing heavy atoms such as Pt should cause significant modifications in the electronic structure. Consequently, we began work on applying the relativistic linearized APW (RLWPW) method[22] to the bulk electronic structure of $PtAs_2$, one of the compounds that appear to be formed in the interaction of Pt contact material with the GaAs substrate. A collaboration with D.D. Koelling (Argonne National Laboratory) was begun and work is continuing on extending RLAPW codes to the pyrite structure of $PtAs_2$.

References

1. G. Samoggia, A. Nucciotti and G. Chiarotti, "Optical detection of surface states in Ge," Phys. Rev. 144, 749 (1966).

2. G. Chiarotti, G. Del Signore, and S. Nannarone, "Optical detection of surface states on cleaved (111) surfaces", Phys. Rev. Lett., 21, 1170 (1968).

3. G. Chiarotti, S. Nanarone, R. Pastore, and P. Chiaradia, "Optical absorption of surface states in ultrahigh vacuum cleaved (111) surfaces of Ge and Si," Phys. Rev. B 4, 3398 (1971).

4. S. M. Sze, Physics of Semiconductor Devices, Wiley-Interscience, New York, 1969, p 406.

5. A. Deneuville and B. K. Chakraverty, "Direct photoelectric measurement of the interface-state density at a Pt-Si interface", Phys. Rev. Lett. 28, 1258 (1972).

6. W. E. Spicer, P. Pianetta, I. Lindau, and P. W. Chye, "Surface and interface states on GaAs (110): Effects of atomic and electronic rearrangements", J. Vac. Sci. Technol. 14, 885 (1977).

7. A. Smith and P. Mark, "Schottky barriers on ordered and disordered surfaces of GaAs (110)", J. Vac. Sci. Technol. 15, 1344 (1978).

8. A. Deneuville, "Characterization of the interface states at a Ag/Si interface from capacitance measurements", J. Appl. Phys. 45, 3079 (1974).

9. S. Kar and W. Dahlke, Solid State Electron. 15, 221 (1972).

10. E. H. Nicollian and A. Goetzberger, "The Si-SiO$_2$ interface-Electrical properties as determined by the metal-insulator-silicon conductance technique", Bell. Syst. Tech J. 46, 1055 (1967).

11. (a) G. P. Alldredge and L. Kleinman, Phys. Rev. Lett. 28, 1264 (1972).
    (b) G. P. Alldredge and L. Kleinman, Phys. Rev. B 10, 559 (1974).

12. (a) E. B. Caruthers, L. Kleinman, and G.P. Alldredge, Phys. Rev. B8, 4570 (1972).
    (b) E. B. Caruthers, L. Kleinman, and G.P. Alldredge, Phys. Rev. B9, 3325 (1974).
    (c) E. B. Caruthers, L. Kleinman, and G.P. Alldredge, Phys. Rev. B9, 3330 (1974).
    (d) E. B. Caruthers, L. Kleinman, and G.P. Alldredge, Phys. Rev. B10,1252 (1974).

13. (a) G. P. Alldredge and L. Kleinman, Phys. Lett. A 48, 337 (1974).
    (b) G. P. Alldredge and L. Kleinman, J. Phys. F: Metal Phys. 4, L207 (1974).
    (c) G. P. Alldredge, in Nuclear Metallurgy, Vol. 20: Computer Simulation for Materials Applications, eds. R.T. Arsenault, J. R. Beeler, and J. A. Simmons (Nuclear Metallurgy Committee, AIME, 1976), p. 582.

14. E.g., R. V. Kasowdki, Phys. Rev. B 14, 3398 (1976), and references therein to earlier work; also, O. K. Andersen, Phys. Rev. B 12, 3060 (1975), and references therein.

15. J. C. Slater and K. H. Johnson, Phys. Rev. B 5, 844 (1972); K. H. Johnson and F. C. Smith, Jr., Phys. Rev. B 5, 831 (1972).

16. E.g., H. Sambe and R. H. Felton, J. Chem. Phys. 62, 1122 (1975); 61, 3862 (1974).

17. E.g., the original non-overlapping muffin-tin form of the MS-Xα gave a minimum of total energy for H_2O at a bond-angle of 180°, versus the experimental bond-angle of 104.6°: J. W. D. Connolly and J. R. Sabin, J. Chem. Phys. 56, 5529 (1972).

18. E.g., J. G. Norman, J. Chem. Phys. 61, 4630 (1974).

19. (a) J.W.D. Connolly, A. Manual for MUSCATEL, Rept. No. 282 (April 25, 1972) and updates (Quantum Theory Project, University of Florida, Gainesville, Florida);
(b) S. Katsuki, P. Palting, and S. Huzinaga, Computer Phys. Commun. 14, 13 (1978).

20. K. H. Johnson and F. C. Smith,Jr., Khem. Phys. Lett. 10, 219 (1971).

21. S. Katsuki, private communication.

22. E.g., D. D. Koelling, in *Proc. 2nd Intl. Conf. Electronic Struct. of Actinides*, J. Mulak, W. Suski, and R. Troc, eds., (Ossolineum, Wroclaw, Poland, 1977), p. 275; D. D. Koelling and G. O. Arbman, J. Phys. F 5, 2041 (1975).

VI. Papers Published 1978 - 79

1. D. L. Begley, R. W. Alexander, C. A. Ward, R. Miller and R. J. Bell, "Propagation distances of surface electromagnetic waves in the far infrared", Surface Sci. 81, 245-51 (1979).

2. D. L. Begley, R. W. Alexander, C. A. Ward and R. J. Bell, "Propagation of surface electromagnetic waves on n-type GaAs in the far infrared", Surface Sci. 81, 238-244 (1979).

3. R. J. Bell, R. W. Alexander, and C. A. Ward, Surface electromagnetic wave spectroscopy in Vibrational Spectroscopies Applied to the Characterization of Adsorbed Species on Catalysts, A. T. Bell, ed. (American Chemical Society, to appear April 1980).

VII. Figure Captions

Fig. 1. The square root of the photoresponse per incident photon plotted against photo energy.

Fig. 2. (a) I-V curve for an Al-GaAs diode with oxygen exposure after cleaving and before metallization. (b) Same on a semi-log plot. The dashed line is for $n = 1.5$.

Fig. 3. Equivalent circuits for diodes with several different oxide thicknesses, t. See text for details.

Fig. 4. Conductance versus bias voltage for an Al-GaAs diode with oxygen exposure after cleaving and before metallization for ⊙, at a frequency of 10 kHz and Δ for a frequency of 20 kHz.

Fig. 5. Equivalent circuits for analyzing capacitance measurements. See text for details.

Fig. 6. Equivalent circuits for analyzing capacitance measurements. See text for details.

Fig. 7. $Cp(\omega_{eq})$, C_{sc} and C_s as a function of bias voltage for an oxygen exposed Al-GaAs diode.

Fig. 8. Density of surface states for an oxygen exposed Al-GaAs diode.

Fig. 9. I-V curve for an Al-GaAs diode metallized immediately after UHV cleave. Straight line is for $n = 1.1$.

Fig. 10. C-V curve for an Al-GaAs diode metallized immediately after UHV cleave.

Fig. 11. I-V curve for an Ag-GaAs diode with oxygen exposure before metallization.

Fig. 12. C-V curve for an Ag-GaAs diode with oxygen exposure before metallization.

Fig. 13. I-V curve for an Au-GaAs diode with oxygen exposure before metallization.

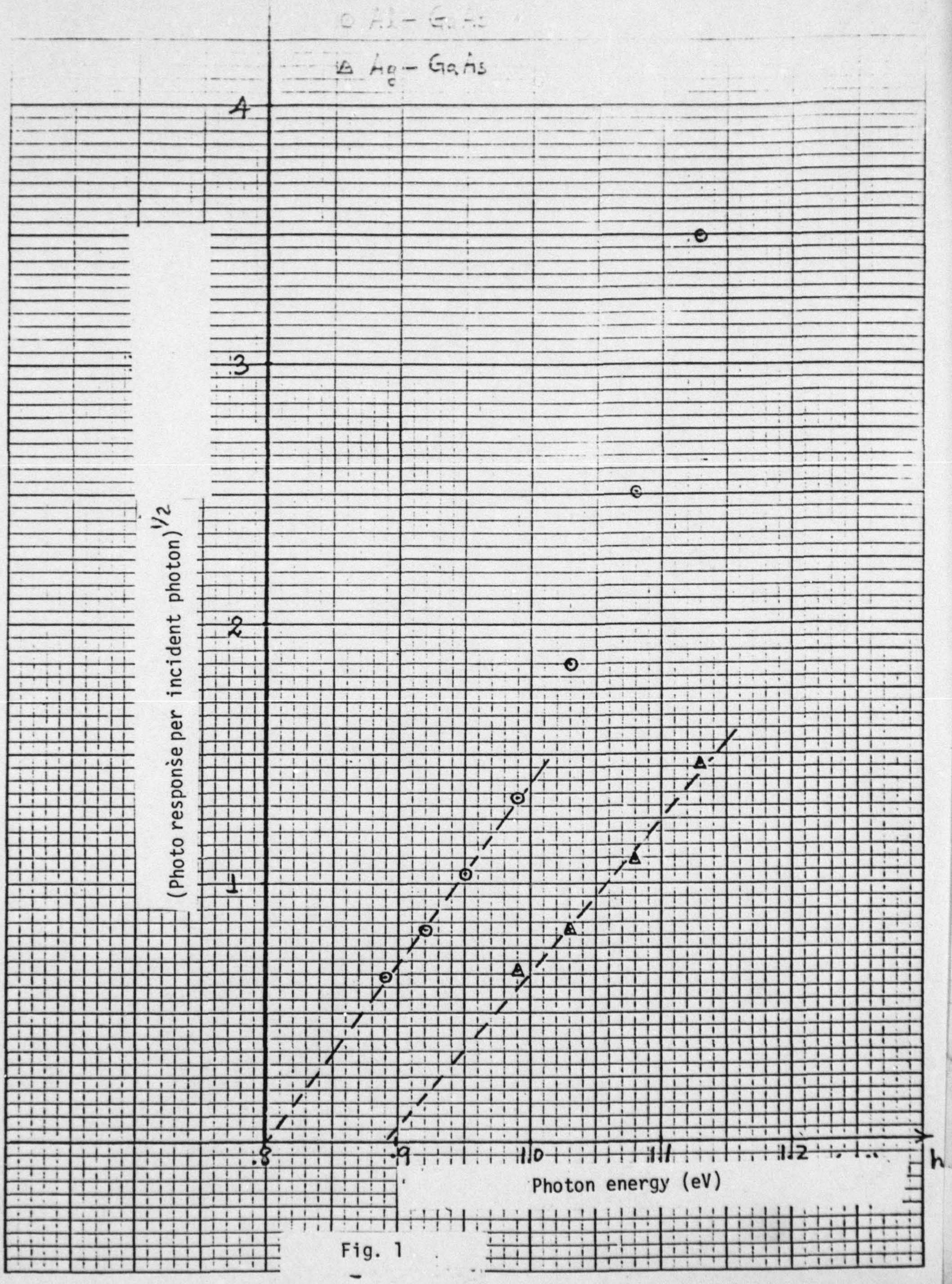
○ Al – GaAs
△ Ag – GaAs
4
3
2
1
(Photo response per incident photon)$^{1/2}$
.8
.9
1.0
1.1
1.2
h
Photon energy (eV)

Fig. 1

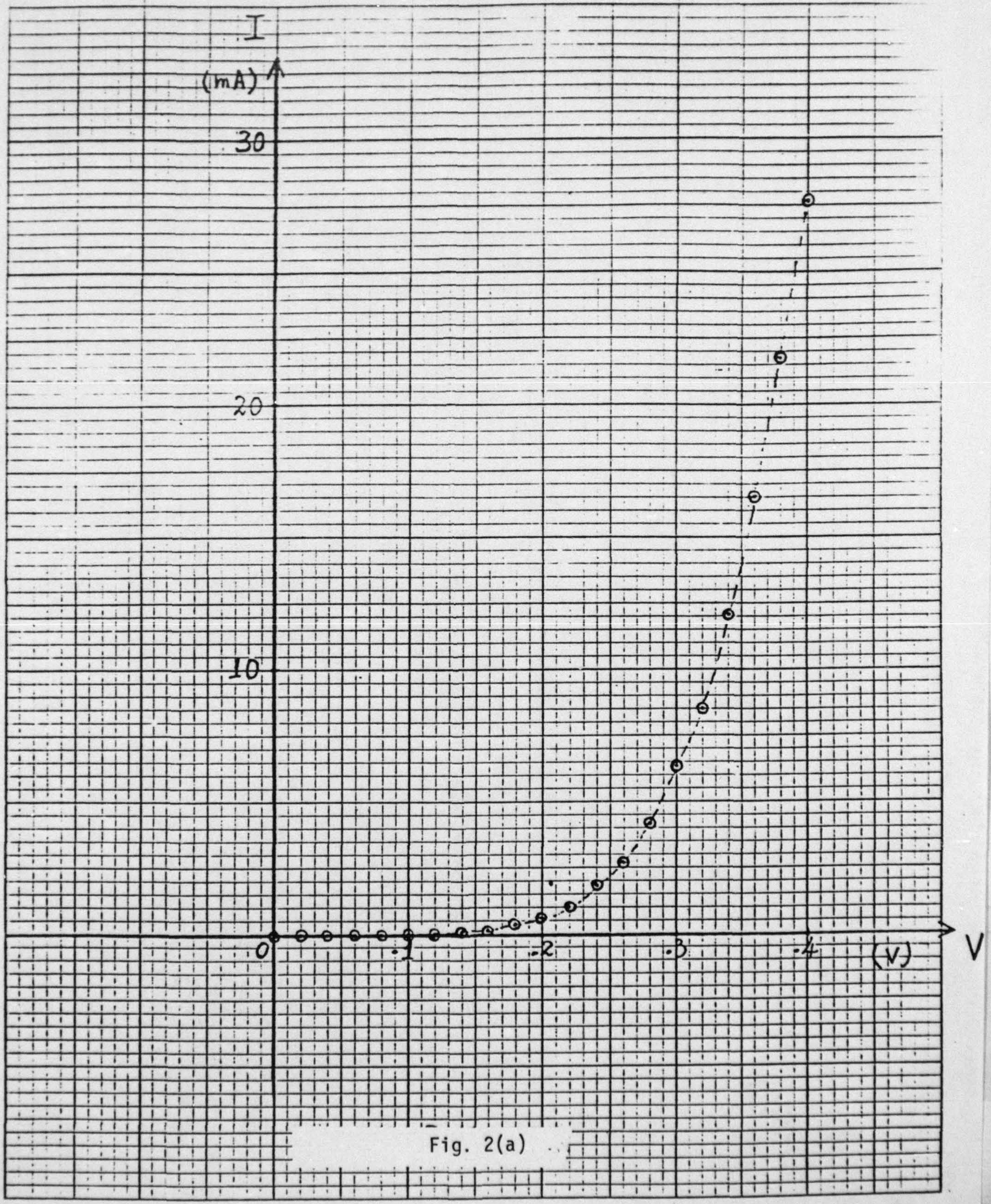

Fig. 2(a)

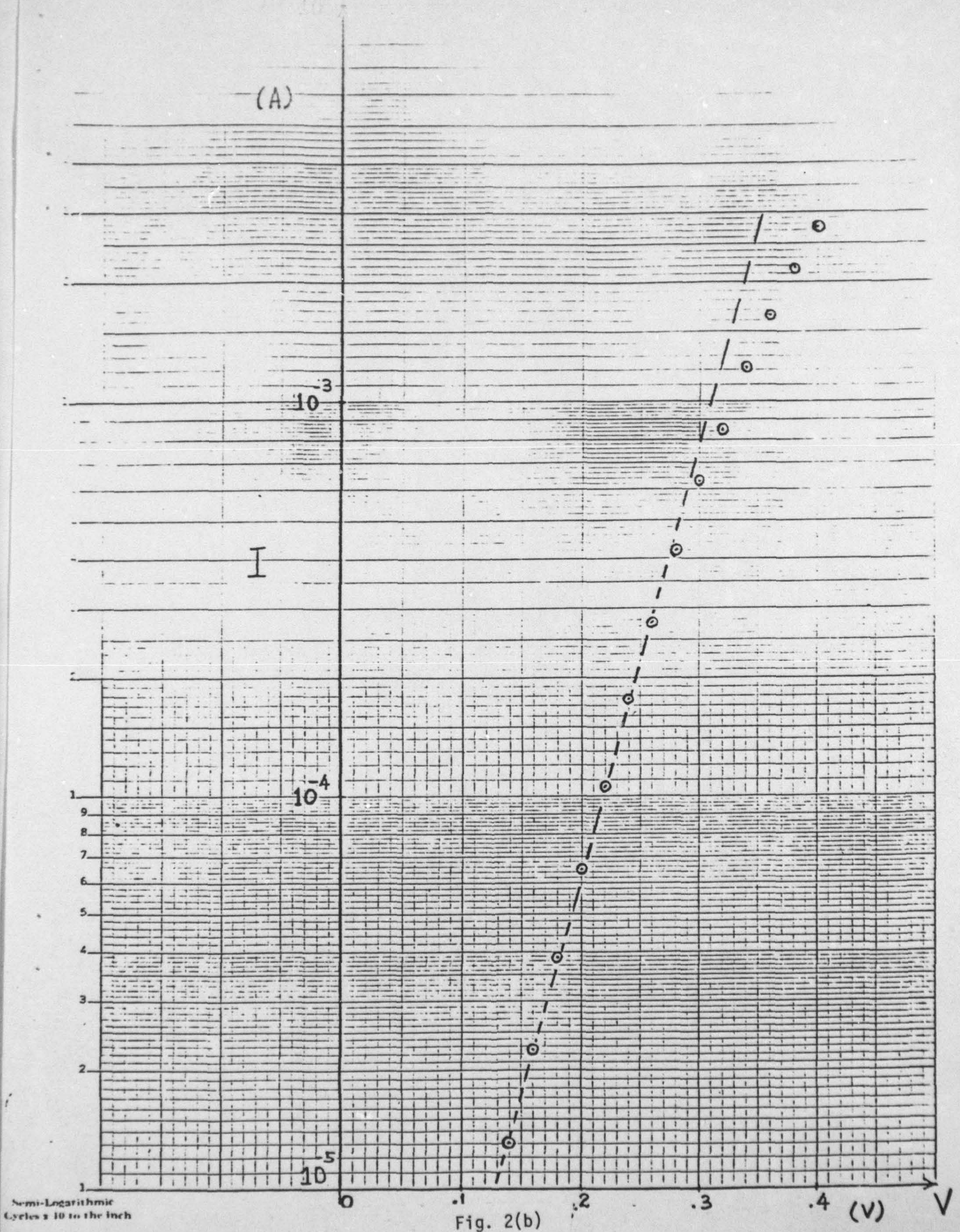

Semi-Logarithmic
Cycles x 10 to the inch

Fig. 2(b)

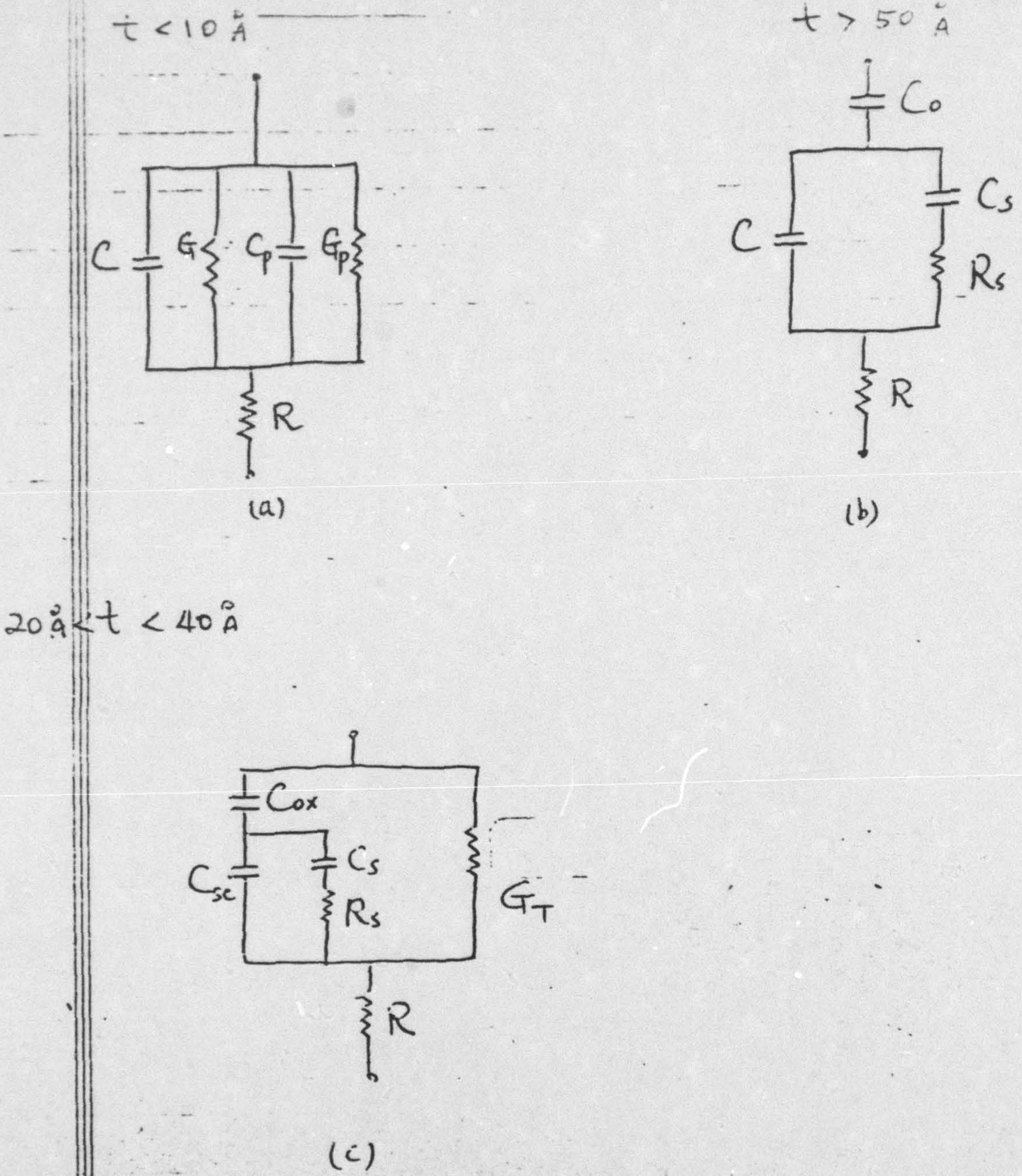

Fig. 3

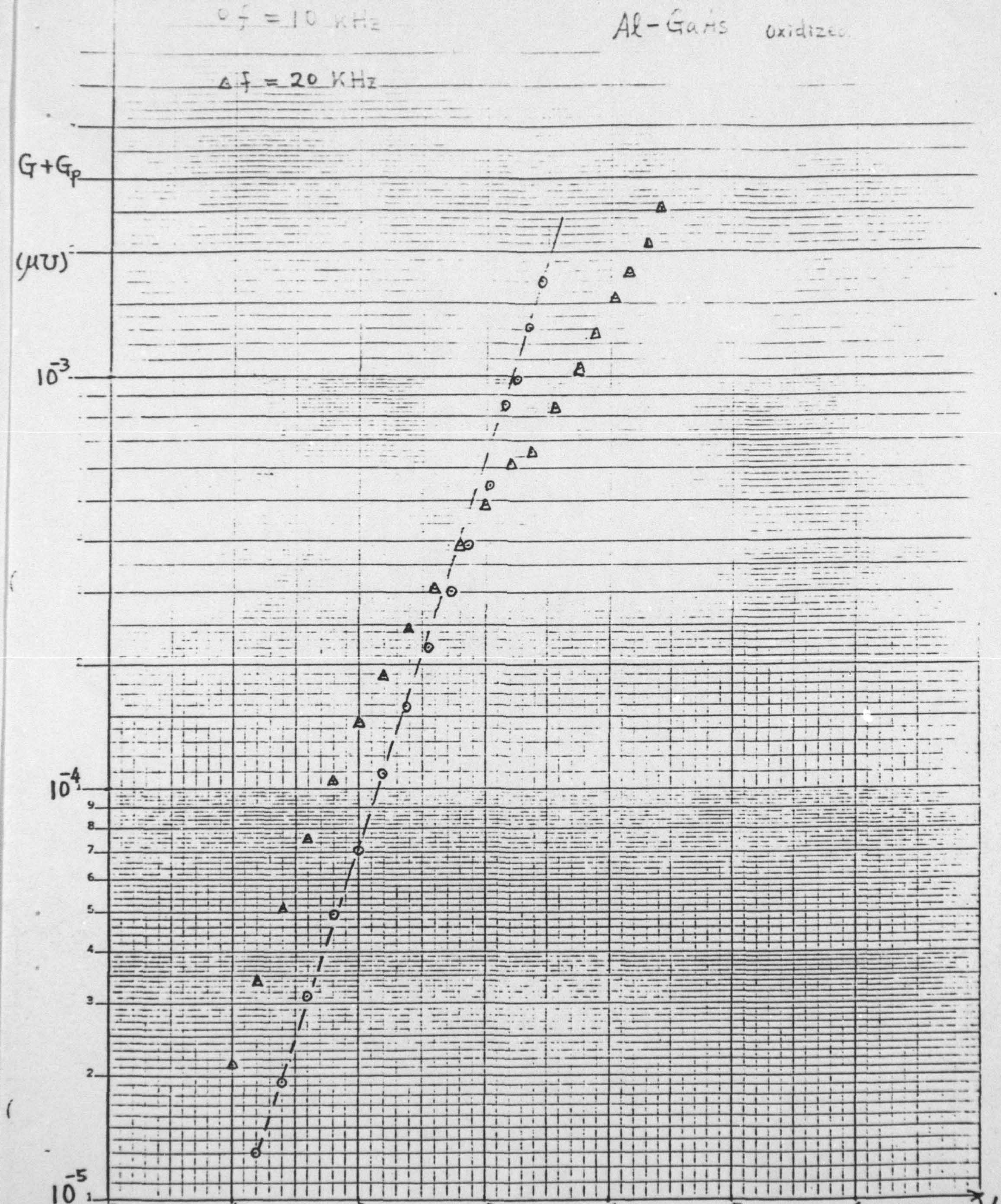
○ f = 10 KHz
△ f = 20 KHz
Al-GaAs oxidized
G+G_p
(μ℧)
10^-3
10^-4
9
8
7
6
5
4
3
2
10^-5 1
0
.1
.2
.3
.4
.5
.6
(V)
V_j
Semi-Logarithmic
3 Cycles x 10 to the inch

Fig. 4

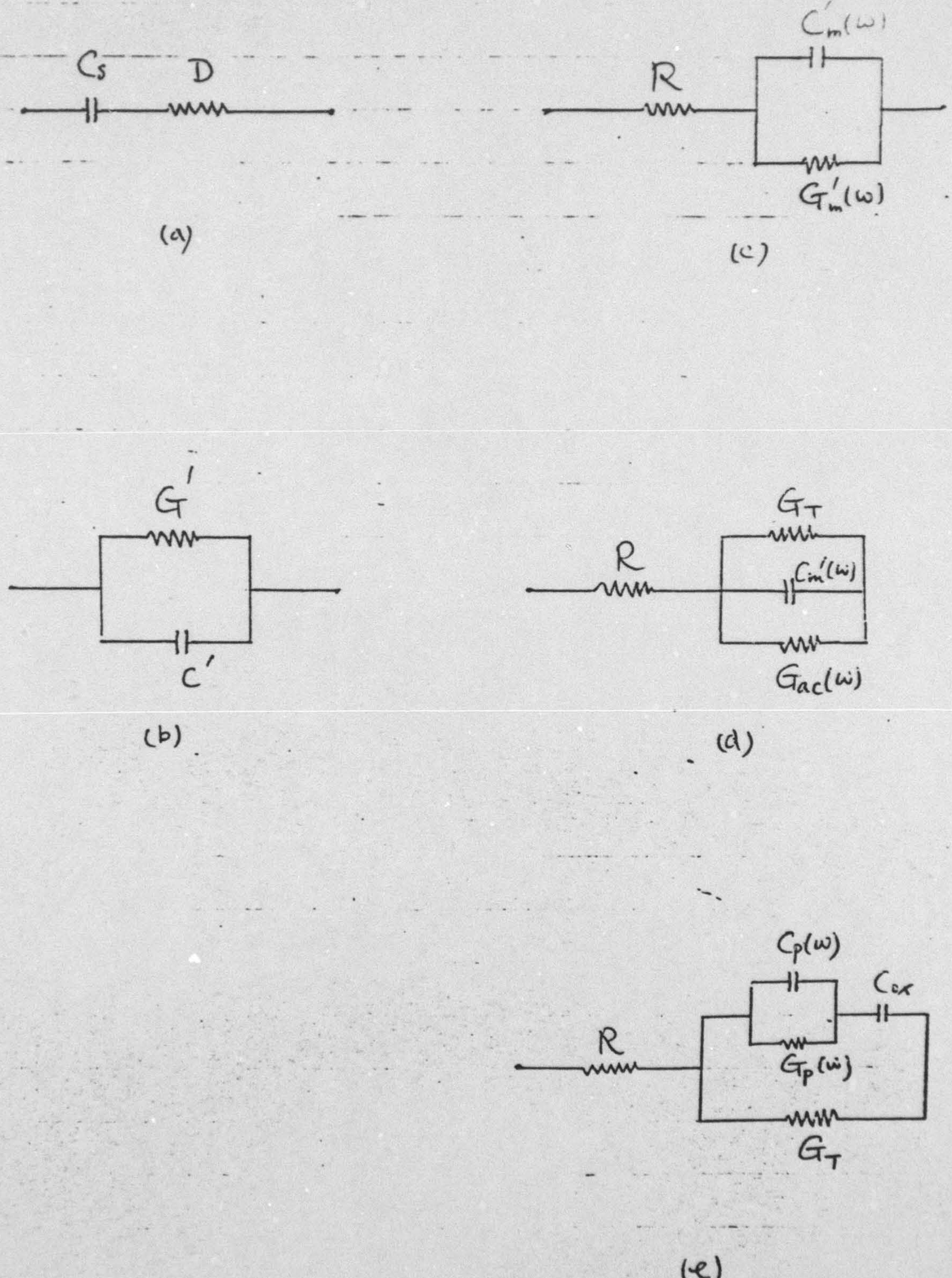
C_s
D
(a)
R
$C_m'(\omega)$
$G_m'(\omega)$
(c)
G'
C'
(b)
R
G_T
$C_m'(\omega)$
$G_{ac}(\omega)$
(d)
$C_p(\omega)$
C_{ox}
R
$G_p(\omega)$
G_T
(e)

Fig. 5

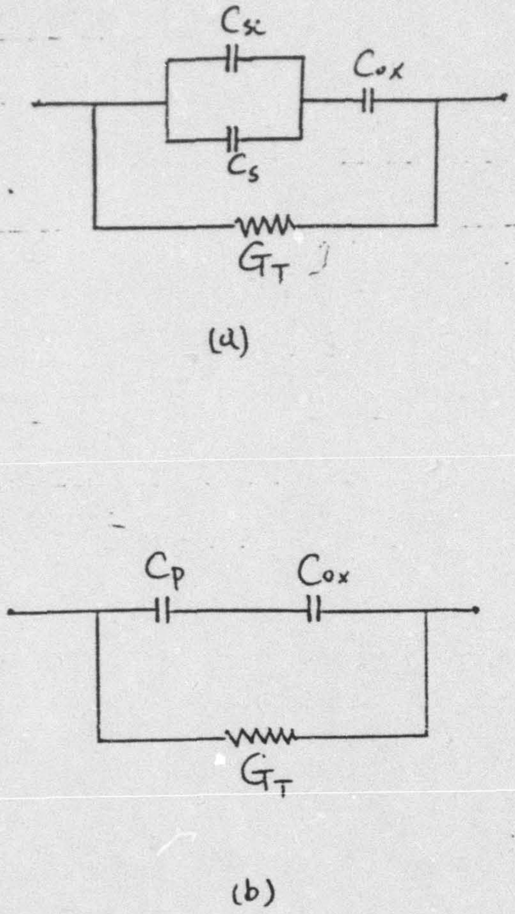

Fig. 6

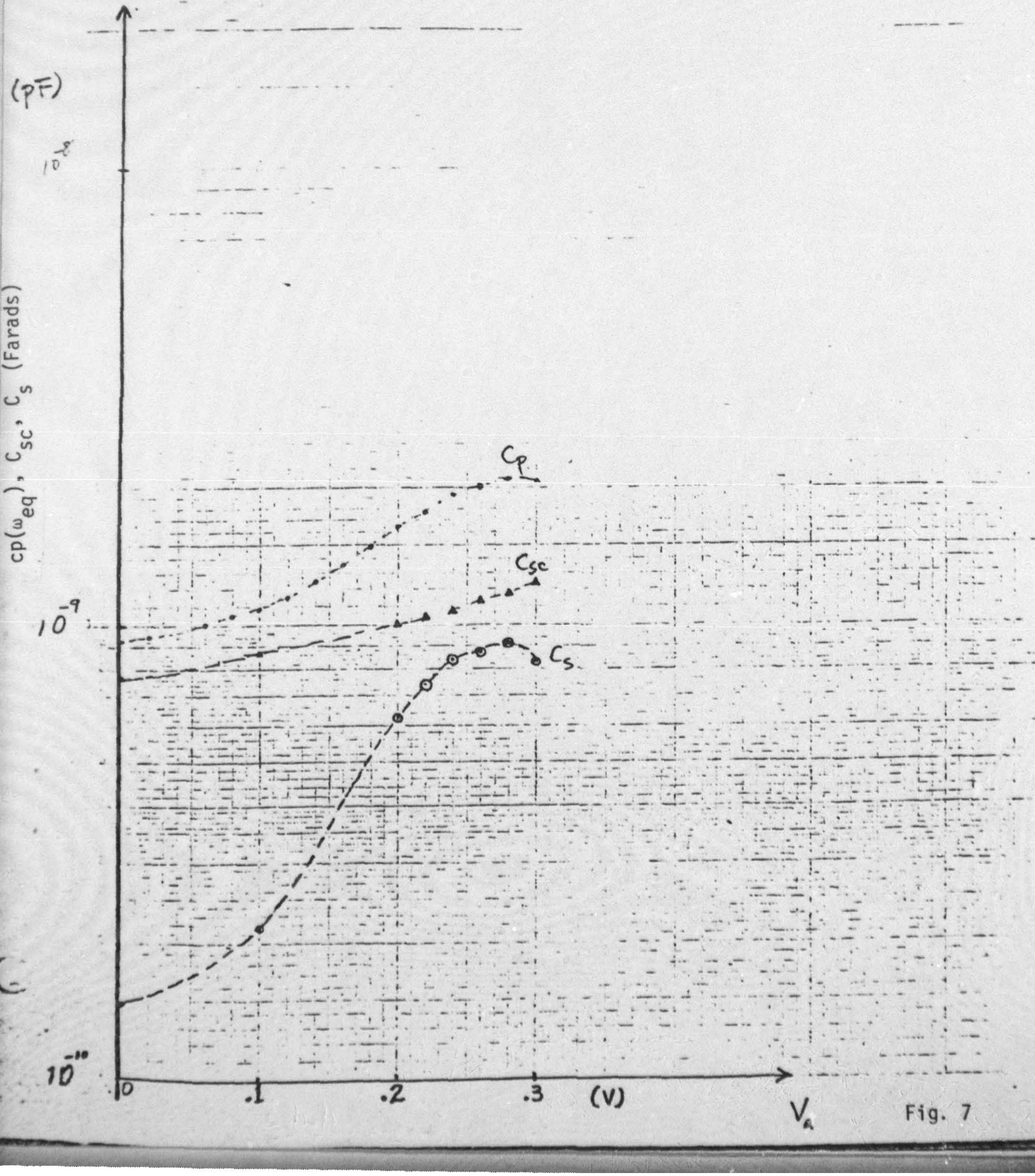

Fig. 7

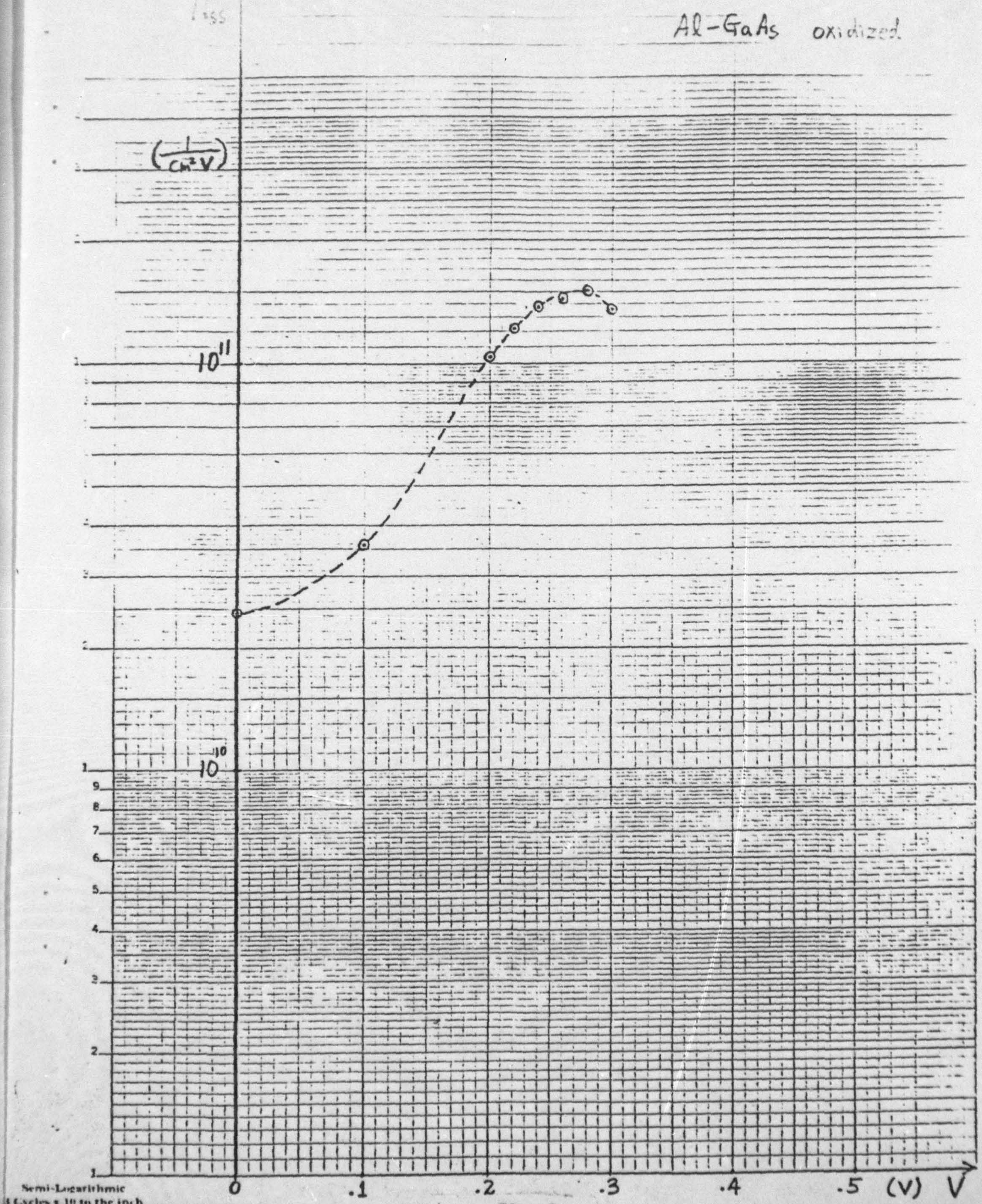
Nss
Al-GaAs oxidized
$\left(\frac{1}{cm^2 V}\right)$
10^{11}
10^{10}
0
.1
.2
.3
.4
.5
(V)
V
Semi-Logarithmic
3 Cycles x 10 to the inch

Fig. 8

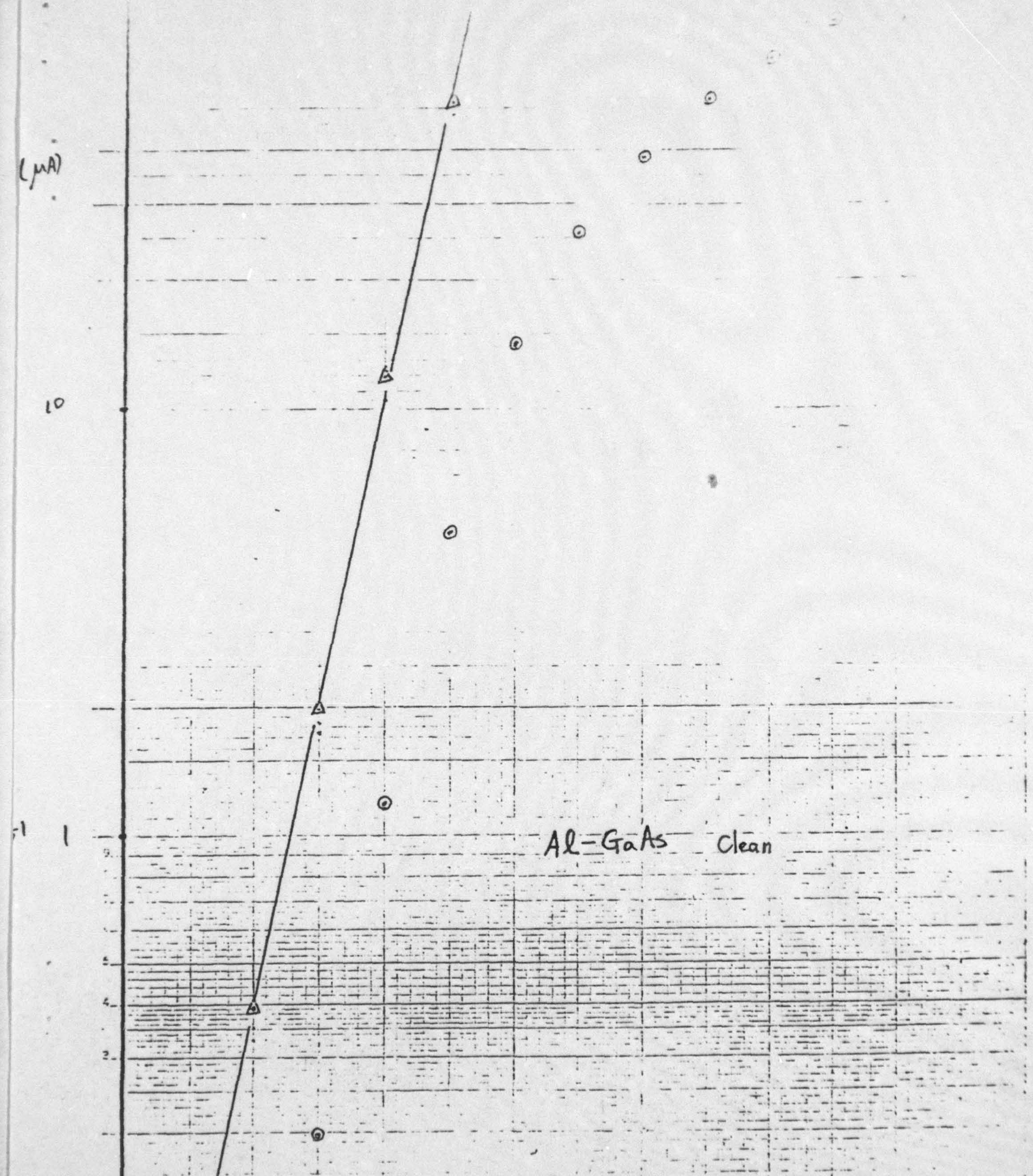

Fig. 9

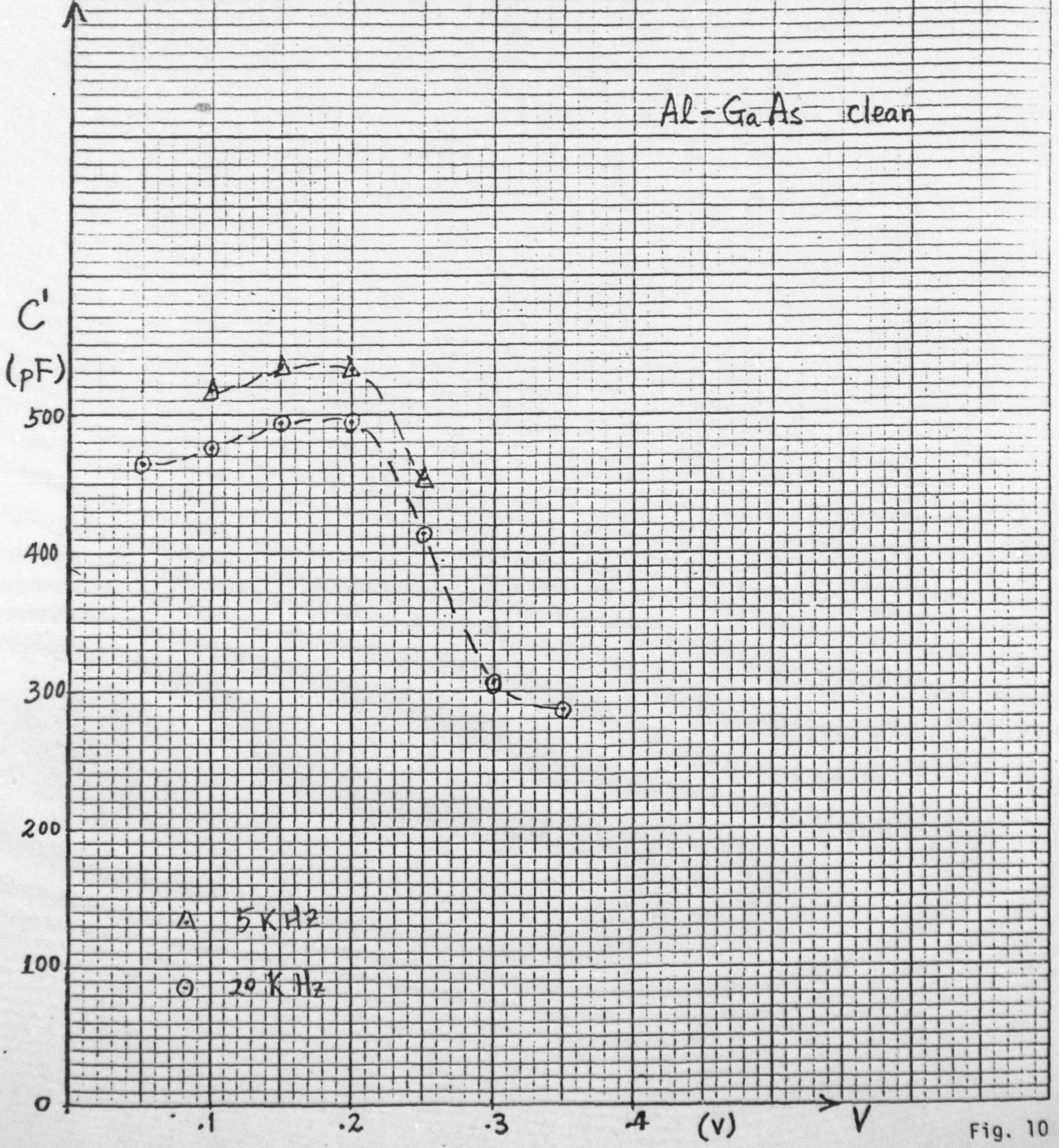

Fig. 10

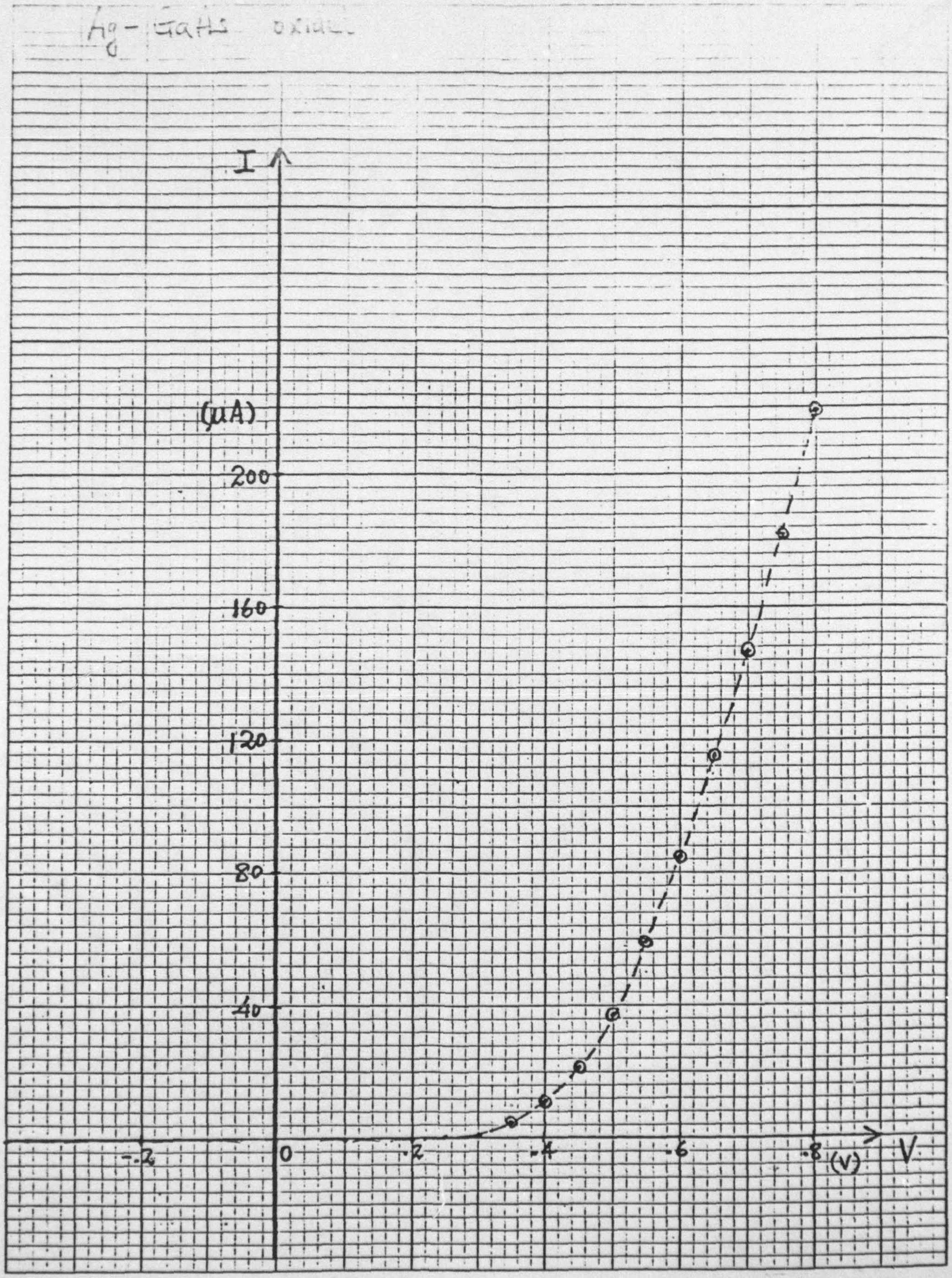

Fig. 11

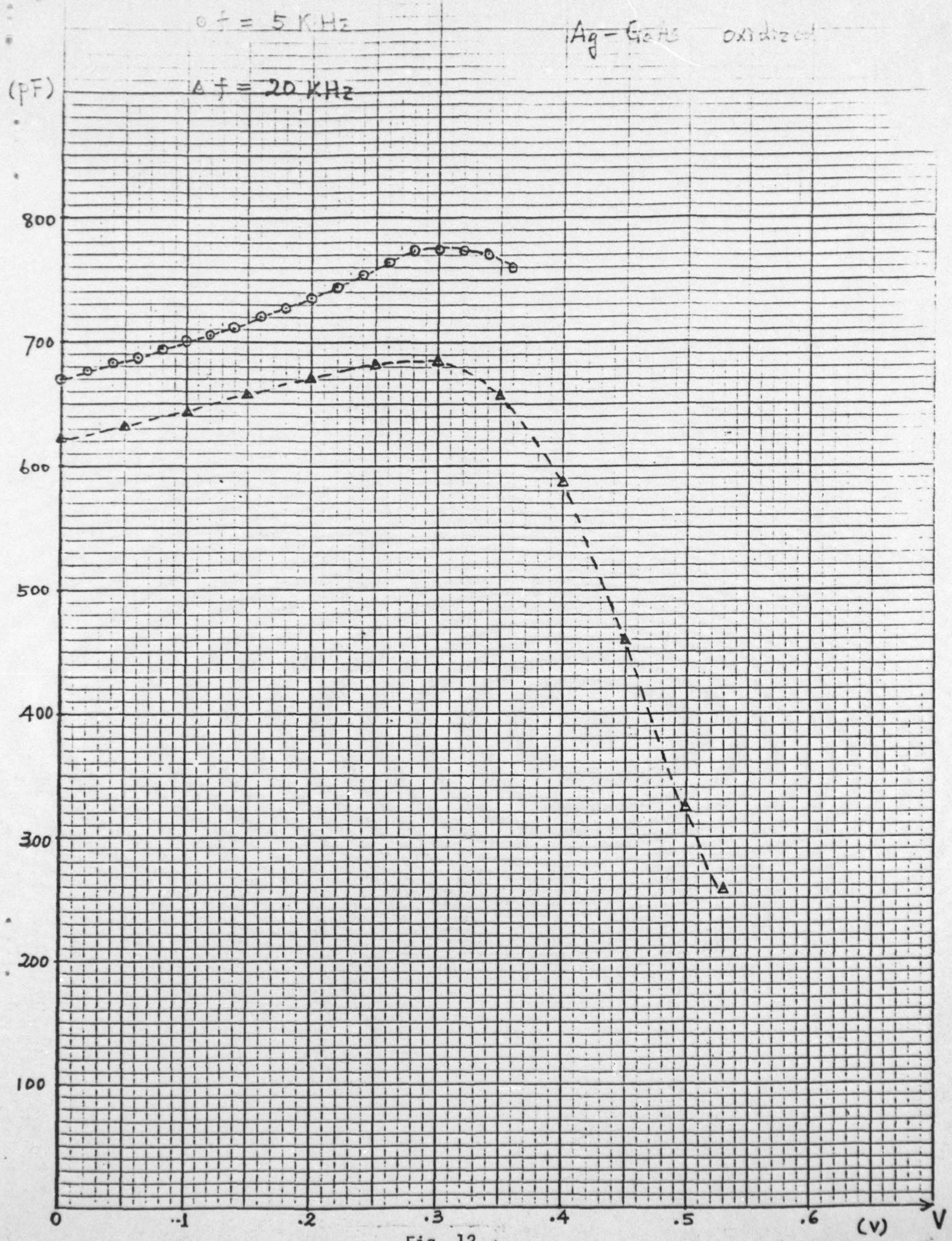
○ f = 5 KHz
Δ f = 20 KHz
Ag – GaAs oxidized
(pF)
800
700
600
500
400
300
200
100
0
.1
.2
.3
.4
.5
.6
(v)
V

Fig. 12

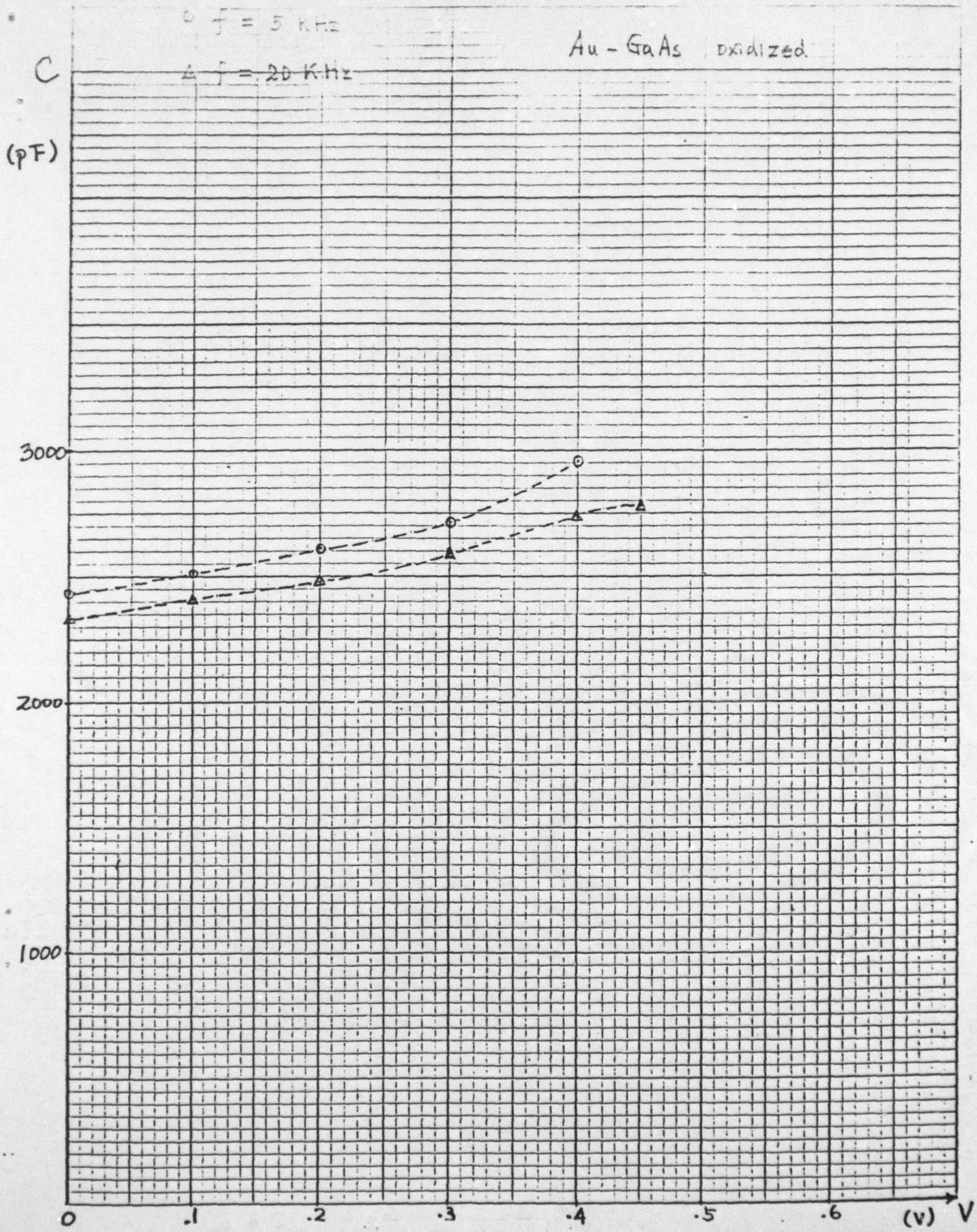

Fig. 13

UNCLASSIFIED

SECURITY CLASSIFICATION OF THIS PAGE (When Data Entered)

18

REPORT DOCUMENTATION PAGE

READ INSTRUCTIONS BEFORE COMPLETING FORM

1. REPORT NUMBER 19
AFOSR-TR- 80-0160

2. GOVT ACCESSION NO.
AD-A083758

3. RECIPIENT'S CATALOG NUMBER

4. TITLE (and Subtitle) 6
Optical Studies of the Interface States at GaAs-Metal Schottky Barrier Junctions

5. TYPE OF REPORT & PERIOD COVERED 9
Final rept.
1 Oct 75 — 29 Sep 78

6. PERFORMING ORG. REPORT NUMBER

7. AUTHOR(s) 10
Robert J. Bell
Ralph W. Alexander, Jr.
Gerald P. Alldredge

8. CONTRACT OR GRANT NUMBER(s) 15
AFOSR-76-2938

9. PERFORMING ORGANIZATION NAME AND ADDRESS
Department of Physics
University of Missouri-Rolla
Rolla, Missouri 65401

10. PROGRAM ELEMENT, PROJECT, TASK AREA & WORK UNIT NUMBERS 16 17
2306/B2
61102F

11. CONTROLLING OFFICE NAME AND ADDRESS
AFOSR/NE
BLDG. # 410
Bolling AFB, DC 20332

12. REPORT DATE 11
1980

13. NUMBER OF PAGES
33

14. MONITORING AGENCY NAME & ADDRESS (if different from Controlling Office)
12 34

15. SECURITY CLASS. (of this report)
UNCLASSIFIED

15a. DECLASSIFICATION/DOWNGRADING SCHEDULE

16. DISTRIBUTION STATEMENT (of this Report)

Approved for public release; distribution unlimited.

DISTRIBUTION STATEMENT A
Approved for public release; Distribution Unlimited

17. DISTRIBUTION STATEMENT (of the abstract entered in Block 20, if different from Report)

18. SUPPLEMENTARY NOTES

19. KEY WORDS (Continue on reverse side if necessary and identify by block number)

20. ABSTRACT (Continue on reverse side if necessary and identify by block number)

The goal of the proposed research was to study surface states at GaAs metal Schottky barrier junctions and the effects of oxygen exposure on the surface states using both optical and electrical measurements with the goal of correlating the optical and electrical results. The correlation could not be achieved because the optical measurements were unsuccessful in detecting the surface states. From the electrical measurements, the following results were obtained: oxygen-exposure before metallization with Al produces a large increase in the surface density of states peaking about 0.28 eV above the Fermi level;

DD FORM 1 JAN 73 1473 EDITION OF 1 NOV 65 IS OBSOLETE

405 701 UNCLASSIFIED

next page

Al—GaAs diodes metallized without oxygen exposure had ideality factors of n equal to less than 1.1; Ag-GaAs diodes with oxygen exposure also show a surface state density peaking about 0.3 eV above the Fermi level. However, the surface state density is considerably lower than for oxygen-exposed AlGaAs dio diodes; Au-GaAs diodes with oxygen exposure show a surface state density which peaks about 0.45 eV above the Fermi level. Again, this density is considerably lower; from the above, oxygen at a GaAs-metal interface plays an important role in determining the surface state density. The theoretical part of this study to calculate electronic energies at GaAs surface was also unsuccessful.